Aerosol-Mediated Fabrication of Porous Thin Films Using Ultrasonic Nebulization

Dominic Walsh,* Laura Arcelli, Vicky Swinerd, Jane Fletcher, and Stephen Mann

Centre for Organized Matter Chemistry, School of Chemistry, University of Bristol, Bristol, BS8 1TS, U.K.

Barbara Palazzo

Departimento di Chimia "G.Ciamician", Universita di Bologna, via Selmi 2, 40126, Bologna, Italy

Received September 14, 2006. Revised Manuscript Received November 15, 2006

High surface area ceramic films and biopolymer films were fabricated by precipitation at room temperature of a reagent aerosol composed of approximately 1 μm diameter microdroplets laid onto a reactive receiver solution using a completely enclosed system. Calcium phosphate films of up to 340 μm in thickness composed of hollow microspheres were generated by gradual settling and precipitation of the reagent microdroplets on the receiver solution surface. Suitability of the ceramic film as a drug support using alendronate as an example was investigated. Chitosan/alginate biopolymer films were similarly prepared and precipitation with limitation to the air/water interface promoted a wire form copper oxide precursor. Zirconia microspheres were prepared without use of surfactant or template via precursor precipitation in a stirred receiver solution. Additional components could be readily incorporated and the flexibility of the novel approach is consistent with a new general strategy for the preparation of thin films and hollow microspheres of nanostructured materials.

Introduction

Nanostructured materials have major technological potential in areas such as catalysis, electronics, magnetism, and biomaterials engineering. Currently, many fabrication routes to nanostructured materials are based on gas condensation and chemical vapor deposition,[1−3] and related techniques such as spray pyrolysis, sputter coating, or spray drying[4−6] use aerosol-assisted procedures to prepare ceramic, metallic, or metal oxide thin coatings. These techniques often require sophisticated electrical, vacuum, and heating procedures, and to address this limitation, we describe in this paper a novel low-temperature fabrication route to nanostructured thin films consisting of ceramic or biopolymeric components. For this, we have developed a facile procedure based on the use of an ultrasonic nebulizer to generate aerosols comprising micrometer-sized droplets of aqueous reagents that are subsequently deposited onto a reactive receiver solution (Figure 1).

We show that reaction of the aerosol droplets at the air/water interface of the unstirred receiver solution produces self-supporting films of inorganic or biopolymeric materials. To illustrate the potential of our new approach, herein we describe in detail studies on the fabrication of thin inorganic films based on calcium phosphate, which has widespread uses in bioceramic implants[7,8] and as a nontoxic support for oral drug delivery.[9,10] We also show how aerosol-assisted interfacial precipitation can be used to prepare thin films of copper hydroxide/oxide and develop the method for the fabrication of soft or mineralized biopolymer films consisting of the polysaccharides, alginate and chitosan. In each case, the film thickness can be controlled by adjustments in the experimental parameters, and under certain conditions, inorganic films with nanoscopic texture and porosity can be produced. In addition, the procedure can be extended to selectively introduce drug molecules into the calcium phosphate films such that composites consisting of spatially segregated domains of guest molecules can be readily fabricated. Similar procedures, but using stirred solutions in

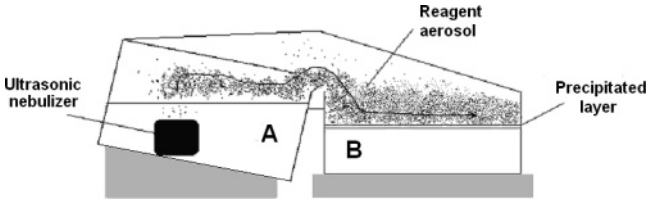

Figure 1. Diagram showing general arrangement of apparatus used in preparation of samples. Aerosol droplets of aqueous solution A are produced by ultrasonic nebulization and directed across the interface of receiver solution B. Typical A/B reaction pairs include calcium nitrate/ammonium hydrogen phosphate, copper nitrate/sodium hydroxide, ammonium hydroxide/zirconia tetraisopropoxide (in propanol), and chitosan/alginate. Aerosols containing drug molecules (such as tetracycline), or Ag nanoparticles, are prepared by nebulization in calcium nitrate or chitosan solutions, respectively.

* To whom correspondence should be addressed. E-mail: d.walsh@bristol.ac.uk.

(1) Herrig, H.; Hempelmann, H. *NanoStruct. Mater.* **1997**, *9*, 241.
(2) Hahn, H. *NanoStruct. Mater.* **1997**, *9*, 3.
(3) Mayo, M. J.; Ciftcioglu, N. *Mater. Res. Soc. Symp. Proc.* **1991**, *206*, 545.
(4) Patil, P. S. *Mater. Chem. Phys.* **1999**, *59*, 185.
(5) Perednis, D.; Gauckler, L. J. *J. Electroceram.* **2005**, *14*, 103.
(6) Madene, A.; Jacquot, M.; Scher, J.; Desobry, S. *Int. J. Food. Sci. Technol.* **2006**, *41*, 1.
(7) Hench L. L. *J. Am. Ceram. Soc.* **1991**, *74*, 1487.
(8) Dorozhkin, S. V.; Epple, M. *Angew. Chem., Int. Ed.* **2002**, *41*, 3130.
(9) Rasenack, N.; Muller, B. W. *Pharm. Dev. Technol.* **2004**, *9*, 1.
(10) Worldwide Patent No. ZA200502693, 2005.

10.1021/cm0621951 CCC: $37.00
Published on Web 01/04/2007

the receiver flask, were developed to produce zirconia microspheres. As the methods are facile, are highly versatile, and do not involve the use of templates or additives, they could be of significant value as fabrication routes to a wide variety of ceramics and polymeric materials for use in numerous applications.

Experimental Section

Calcium Phosphate Film Preparation. Calcium phosphate films were produced as follows. Aqueous $Ca(NO_3)_2{\cdot}4H_2O$ (1 L, 0.5 M) was placed in a 1.5 L evaporating basin tilted at an angle to the horizontal. The solution was subjected to ultrasonic nebulization using a small nebulizer unit immersed in the solution to produce aerosols consisting of ~1 μm sized aqueous droplets at a rate of ~90 mL h^{-1} (Stowasis SMG 0109 ultrasonic nebulizer, 18 mm diameter nebulizing ceramic membrane). A glass plate was used to cover most of the basin which served to prevent direct transfer of large droplets. The whole system was completely enclosed and the mist produced was directed over a separate flask containing 500 mL of 0.3 M $(NH_4)_2HPO_4$ (pH 8.2) for periods up to 5 h, during which nearly all of the droplets generated gradually settled onto the receiver solution. To obtain films of uniform thickness, the receiver solution could be rotated by 180° at the midpoint of the deposition period. Calcium phosphate films were collected at the air/water interface of the $(NH_4)_2HPO_4$ solution by filtration, washed with distilled water, and air-dried. Typically, a final yield of ~1.4 g was obtained after 4 h of deposition. (Note: It was observed that, unlike solutions of $Ca(NO_3)_2{\cdot}4H_2O$, aqueous $CaCl_2$ solutions did not undergo ultrasonic nebulization to form stable aerosols.)

A carbonated HAP film was also prepared as above except that a 0.195 M $(NH_4)_2HPO_4$ and 0.105 M Na_2CO_3 solution (pH 8.7) was used as the receiving solution.

Copper Hydroxide/Oxide Films. Similar procedures were used to prepare thin films of copper oxide. An aerosol mist prepared by nebulization of an aqueous solution of $Cu(NO_3)_2{\cdot}2.5H_2O$ (0.25 M, 1 L) was allowed to interact with an unstirred NaOH solution (0.2 M, 1 L) for 3 h. The resulting film was heated subsequently to 500 °C at a rate of 10 °C min^{-1} to produce CuO granules.

HAP/Drug Composite Films. A HAP (or carbonated HAP) film was prepared as above using an aerosol-mediated deposition time of 120 min. The calcium nitrate solution was then replaced by a 0.5 M aqueous $Ca(NO_3)_2{\cdot}4H_2O$ solution containing tetracycline (0.5 g/100 mL), which was then subjected to ultrasonic nebulization. The generated mist was directed over the phosphate receiver solution containing the floating HAP film for 60 min to produce a HAP/tetracycline overlayer. The Ca^{2+}/ tetracycline solution was then replaced with aqueous 0.5 M $Ca(NO_3)_2{\cdot}4H_2O$, which was then used to deposit a third layer at the air/water interface of the phosphate receiver (reaction time, 90 min). The final film was collected as above.

Absorption of alendronate (sodium trihydrogen (4-amino-1-hydroxybutylidene) diphosphonate trihydrate) to prepared HAP films was determined by measurement of the residual alendronate concentration in solution by an indirect spectrophotometric method as previously reported.[11] Ten milligrams of the prepared HAP film was added to 1.5 mL of ultrapure water containing 3 mg mL^{-1} alendronate. The vessel was then held in a shaking incubator for 120 min at 37 °C. At scheduled times for up to 11 days, aliquots (100 μL) of the supernatant, separated from the solid phase by centrifugation, were removed for drug quantification and replaced with fresh water. Residual alendronate was measured by reaction with ninhydrin followed by spectrophotometric measurement at 568 nm.

Preparation of Zirconia Hollow Microspheres. Hollow microspheres of $Zr(OH)_4$ were prepared by directing a nebulized aerosol generated from a 1 L solution of deionized water containing 5 mL of $NH_4(OH)$ onto a dish containing 5 mL of a 70% propanol solution of $Zr(OC_3H_7)_4$ diluted in 300 mL of ethanol (0.0112 g of $Zr(OC_3H_7)_4$/mL of ethanol) for a period of 30 min. The receiving dish was stirred at moderate speed with a magnetic stirring bar. After 30 min of aerosol deposition, the suspended white product was collected by filtration, washed with 100% ethanol, and air-dried, giving a yield of ~2.2 g. The collected material was then converted to ZrO_2 by heating to 750 °C at 10 °C min^{-1} in a furnace with a dwell time of 30 min.

Chitosan/Alginate Films. Chitosan/alginate films mineralized with calcium phosphate were fabricated by modification of a published method for the preparation of mineralized polysaccharide microspheres.[12] Briefly chitosan (0.25 wt %) was dissolved in 1 L of a 0.25% solution of acetic acid containing 12.5 mM $CaCl_2$. A nebulized aerosol of this solution was deposited for 2 h onto 500 mL of 0.5 wt % sodium alginate in NaCl (0.04M) containing 25 mM Na_2HPO_4. The precipitated films were robust and could be lifted from the receiver solution surface and stored in distilled water as flexible sheets.

Mineralized chitosan/alginate films were also prepared with silver nanoparticles by addition of 10 mL of a silver colloid to the chitosan solution prior to ultrasonic nebulization. The silver nanoparticles were prepared by dissolving 0.1 g of $AgNO_3$ in 15 mL of deionized water and mixing this solution with 30 g of dextran (Mr 6000, Fluka). The mixture was covered and stored overnight. Reduction of the salt to metallic silver was promoted by the terminal aldehyde groups of the dextran polymer chains, while the overall viscosity of the reaction solution inhibited crystal growth. Ascorbic acid was then added to reduce any unreacted $AgNO_3$ and the mixture centrifuged at 5000 rpm for 20 min. The Ag content of the supernatant was 5×10^{-4} g mL^{-1} (gravimetric analysis), and the particles were ca. 200 nm in size (SEM results).

Characterization. SEM microscopy of samples mounted on aluminum stubs and sputter-coated with Pt/Pd was conducted using a Jeol 6330 field emission SEM operating at 10 keV and 12 μA and a Jeol 5600 SEM operating at 15 keV. Samples analyzed by EDXA analysis were sputter-coated with carbon. XRD was conducted using a Bruker D8 advance powder diffractometer at 40 keV (Cu $K\alpha_1$ radiation 1.5405 Å; 2θ values 2.00−60.00° with step interval of 0.04°). All samples were hand-ground before analysis. Surface area was measured using a Carlo Erba Sorpty 1750 BET analyzer at constant volume N_2 absorption with desorption at 200 °C. Fourier transform infrared (FT-IR) samples were analyzed as KBr disks on a Perkin-Elmer Spectrum One spectrometer.

Results and Discussion

Thin, self-supporting white films of hydroxyapatite ($Ca_{10}(PO_4)_6(OH)_2$, HAP) or carbonated HAP (which has a higher solubility than pure HAP and therefore often preferred in biomaterial applications) were produced by directing a mist consisting of micrometer-sized aerosol droplets of aqueous $Ca(NO_3)_2$ onto the air/water interface of an unstirred aqueous solution of $(NH_4)_2HPO_4$ at pH 8.2 (or $(NH_4)_2HPO_4/Na_2CO_3$

(11) Taha, E. A.; Youssef, N. F. *Chem. Pharm. Bull.* **2003**, *51*, 1444.

(12) Green, D. W.; Leveque, I.; Walsh, D.; Howard, D.; Yang, X.; Partridge, K.; Mann, S.; Oreffo, R. O. C. *Adv. Funct. Mater.* **2005**, *15*, 917.

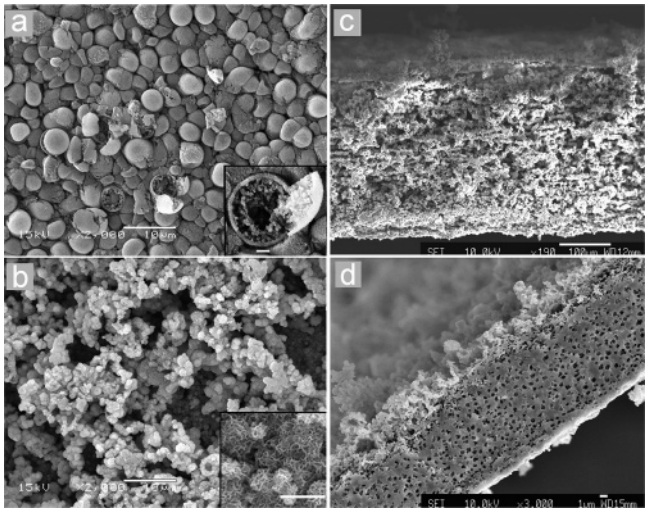

Figure 2. SEM micrographs: (a) Underside (solution-facing) of HAP film showing randomly packed hollow hemispheres, scale bar = 10 μm; inset shows broken sphere with hollow interior, scale bar = 1 μm. (b) Top surface of HAP film showing disordered open network of hollow spheres, scale bar = 10 μm; inset shows high-resolution image of microsphere showing highly texture surface, scale bar = 1 μm. (c) Cross section of HAP film formed after 4 h showing sublayering after drying, scale bar = 100 μm. (d) Cross section of carbonated HAP film produced after 2 h showing a continuous inorganic matrix and well-dispersed voids, scale bar = 100 μm.

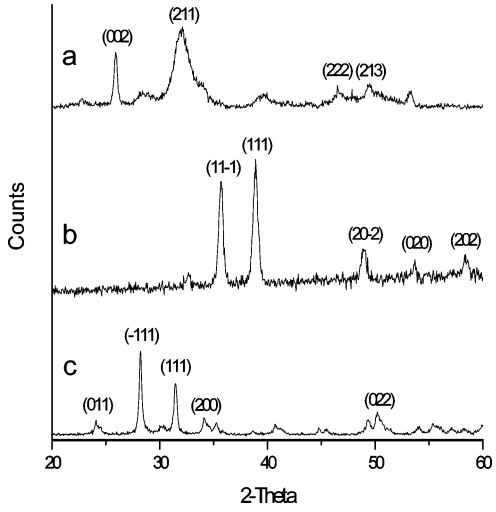

Figure 3. XRD diffraction spectra of samples prepared by aerosol-mediated deposition: (a) HAP film formed after 4 h, (b) CuO obtained after heating $Cu(OH)_2$ film at 500 °C, and (c) ZrO_2 hollow microspheres obtained after heating $Zr(OH)_4$ particles at 750 °C.

at pH 8.7, respectively) for periods up to 5 h (see Experimental Section). Precipitation of the inorganic phase occurred specifically at the air/water interface such that the phosphate solution below the deposited layer remained completely clear. The film progressively increased in thickness and coherence with time to produce a continuous layer with a maximum thickness of ~340 μm after approximately 4 h of aerosol deposition. Thicker films were not supported by the surface tension of the phosphate solution and descended to the bottom of the container, with the consequence that a new layer of precipitate was initiated at the air/water interface.

Intact films could be removed from the air/water interface provided that they were handled with care. The film surface in contact with the solution was composed of a random array of packed hemispheres, ca. 5 μm in diameter (Figure 2a), while the top (air-facing) surface was highly irregular and porous and consisted of an open framework of aggregated particles with diameters of around 2 μm (Figure 2b). SEM images of broken spheres present on the underside of the film showed that the particles were hollow with a spongelike interior texture surrounded by a continuous wall, 200−300 nm in thickness (Figure 2a inset). High-resolution images indicated that the surface of the microspheres was extensively crumpled on a length scale of 50−100 nm (see Figure 2b inset). This was consistent with the high surface area of 155 $m^2\ g^{-1}$ measured by BET analysis. Powder X-ray diffraction (XRD) of the films showed broad reflections at 3.44, 2.80, 2.26, 1.95, 1.84, and 1.72 Å corresponding to the (002), (211), (310), (222), (213), and (004, 411) *d* spacing of poorly crystalline HAP (JCPDS card 9-432) (Figure 3a).

In general, the calcium phosphate films increased in thickness by aggregation and packing of hollow microspheres that continued to form at the air/water interface. In this regard, the pH of the receiving solution and formation of a porous layer at the interface were important factors in enabling thicker films to be produced. Whereas porous films were readily prepared using a receiver solution of aqueous $(NH_4)_2HPO_4$ at pH 8.2, experiments using Na_2HPO_4 at pH 9.2 produced films of increased density and thinness due to faster rates of calcium phosphate nucleation and growth under these conditions. Moreover, SEM images of samples viewed in a cross section indicated that the dried HAP films consisted of substructural layers that were approximately 15 μm in thickness (Figure 2c). Along with the crumpled texture of the mineral particles, this self-organized layering was most likely the result of the redistribution and shrinking of the spheres on drying, although it could serve a useful role in reducing crack propagation across the film. In contrast, dried films of carbonated HAP did not show a layered substructure in the cross section. Instead, a matrix consisting of a continuous inorganic matrix and evenly distributed well-defined voids was observed (Figure 2d), suggesting that extensive fusion of the hollow mineral particles along with in-filling of any interstitial spaces between the aggregated spheres occurred throughout the deposited film. This was consistent with the increased level of mineralization associated with the slightly higher pH used to prepare the carbonated HAP films.

As calcium phosphate is extensively used as a nontoxic support for numerous water-insoluble biomolecules, we investigated the scope of using the above HAP films in association with their high surface area and nanotexture for the adsorption and release of various drug molecules. As proof of principle, we prepared HAP or carbonated HAP films directly in the presence of the antibiotic tetracycline[11,12] and in addition used preformed films as porous supports for the osteoporosis bisphosphonate drug alendronate.[13−16] In the former approach, we prepared a three-layered composite film

(13) Dash, A. K.; Cudworth, G. C. *J. Pharmacol. Toxicol. Methods* **1998**, *40*, 1.
(14) Shirtliff, M. E.; Calhoun, J. H.; Mader, J. T. *Clin. Orthop. Relat. Res.* **2002**, *401*, 239.
(15) Seam, C. S. *The complete drug reference*; Pharmaceutical Press: U.K., 2002; p 744.
(16) Reid, D. M. *Bone* **2006**, *38*, S18.

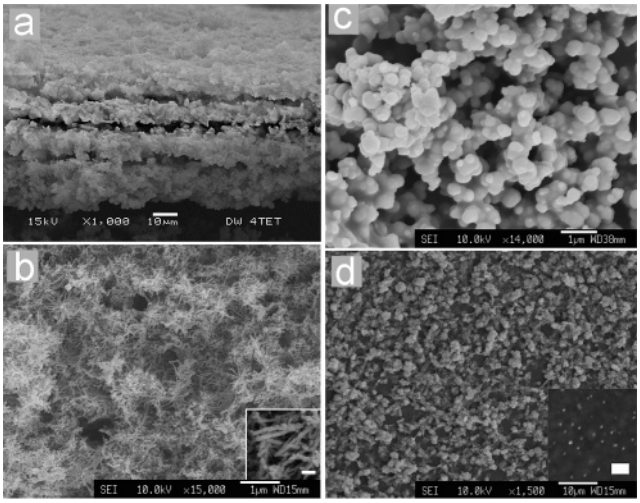

Figure 4. SEM micrographs: (a) Cross section of sequential deposited three-layer HAP/tetracycline composite film: the middle layer containing the intercalated drug molecule is clearly visible, scale bar = 10 μm. (b) Granules composed of nanofilaments of CuO crystals obtained after heating an aerosol-deposited film of $Cu(OH)_2$ at 500 °C; inset shows enlargement of CuO nanofilaments, scale bar = 100 nm. (c) ZrO_2 microspheres obtained by aerosol-deposited $Zr(OH)_4$ particles following heat treatment at 750 °C, scale bar = 1 μm. (d) Top face of mineralized chitosan/alginate/Ag nanoparticle film showing incipient calcium phosphate/polysaccharide spheroids, scale bar = 10 μm; inset shows film underside (solution-facing) with embedded Ag nanoparticles clearly visible, scale bar = 2 μm.

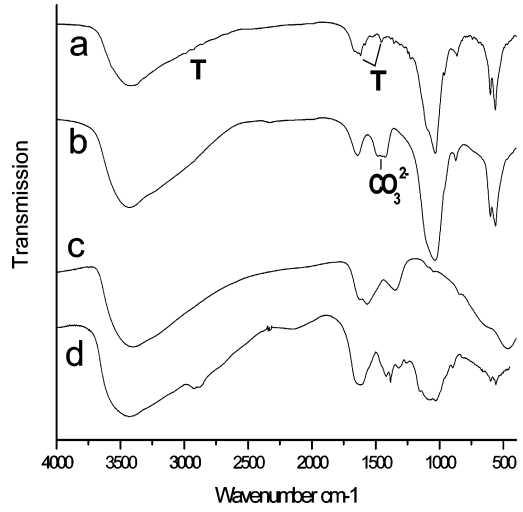

Figure 5. FT-IR spectra of prepared samples: (a) HAP film containing tetracycline (T), (b) carbonated HAP film showing CO_3^{2-} absorption band, (c) $Zr(OH)_4$ microspheres, and (d) mineralized chitosan/alginate/silver film.

by sequential interfacial deposition of aerosol droplets containing Ca^{2+}ions in the presence or absence of tetracycline (see Experimental Section). The intact composite film consisted of a middle HAP-tetracycline yellow layer sandwiched between two pure HAP layers (Figure 4a).

Typically, the nanostructured carbonated HAP films had surface areas of the order of 145 $m^2\ g^{-1}$. FT-IR spectra (Figure 5a) showed characteristic HAP phosphate bands at 563, 602, and 1035 cm^{-1}, a carbonate absorbance at 1450 cm^{-1}, and a peak for absorbed water at around 1620 cm^{-1} and a broad OH band at 3420 cm^{-1}. In addition, bands associated with intercalated tetracycline were observed as a shoulder at 1680 cm^{-1} on the absorbed H_2O band (cyclic C═O) and around 2900 cm^{-1} (CH). Alternatively, we used pre-prepared HAP films as a support for the absorption of

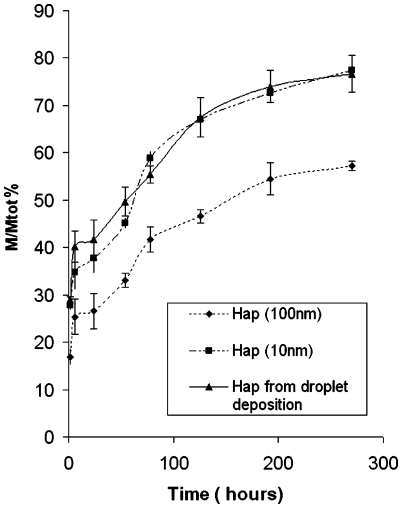

Figure 6. Plots showing absorption profiles over 300 h for alendronate in the presence of aerosol-deposited HAP film (◆), 10 nm sized HAP particles (■), and 100 nm sized HAP particles (▲). M = mass of drug absorbed onto HAP, M_{tot} = total weight of drug in solution.

sodium alendronate from aqueous solution. The adsorption profiles, which were recorded over a period of 11 days, showed an initial uptake of ca. 30%, followed by a progressive increase in the amount adsorbed to a value of 80% after 300 h (Figure 6). The uptake properties were similar to and significantly better than those measured for HAP powders consisting of 10 and 100 nm sized particles, respectively (Figure 6), consistent with the nanostructured surface texture of the HAP films.

To illustrate the scope of ultrasonic nebulization as a facile method for preparing thin films of metal oxides, mists of aqueous copper nitrate were generated and directed onto the air/water interface of aqueous NaOH (see Experimental Section). Thin self-supporting films of $Cu(OH)_2$ were produced within 3 h. Significantly, the films could be removed and thermally transformed to copper oxide. SEM images showed that both the unheated and heat-treated materials consisted of an interconnected matrix of filaments that were 500 and 50 nm in length and width, respectively (Figure 4b). The heated sample had a measured surface area of 36 $m^2\ g^{-1}$, and XRD profiles showed major reflections at 2.52, 2.32, 1.86, 1.71, and 1.58 Å corresponding to the $(11\bar{1})$, (111), $(20\bar{2})$, (020), and (202) d spacings of monoclinic CuO (ICDD card 48-1548) (Figure 3b). In contrast, control preparations using bulk mixing of the reagents at the same concentration produced an aggregated roughly spherical crystalline product after heating, and SEM observations showed no evidence of fiber growth. The results suggested that filament growth was promoted specifically by constraints in microdroplet diffusion and precipitation at the air/water interface of the NaOH solution. Unlike in bulk solution, aerosol-mediated deposition was constrained by the gradual introduction of moderately low concentrations of Cu(II) ions and confined in two dimensions by reaction at the air/water interface of the receiver solution, both of which appear to promote anisometric crystal development of the initially nucleated crystals.

As expected, stirring the receiver solution did not produce intact self-supporting films. Instead, a range of structures

were obtained depending on the stirring rate. For example, hollow spheres of calcium phosphate that decreased in diameter with increasing stirring speed were obtained at moderate rates of mixing, while at high stirrer speeds unusual mushroom-shaped particles up to 10 μm in length were formed (data not shown). We adapted this procedure to fabricate hollow ceramic particles for possible applications in catalysis, drug delivery, enzyme, or DNA stabilization.[17−19] Specifically, we used ultrasonic nebulization to generate a mist of water droplets that were directed against the air/water interface of a stirred Zr(IV) alkoxide solution in propanol. A cloudy suspension was rapidly formed, which was shown by XRD to consist of amorphous $Zr(OH)_4$ (broad XRD reflection at $2\theta = 30°$). FT-IR spectra showed typical Zr−O and OH bands at 465 and 3404 cm^{-1}, respectively, together with absorbed CO_2 bands at 1350, 1565, and 1622 cm^{-1} [20] (Figure 5c). SEM observations of the unheated samples, as well as powders produced after heat treatment at 750 °C, showed microspheres with diameters between 0.5 and 2 μm (Figure 4c); occasional broken microspheres revealed a hollow interior to the microspheres. XRD analysis of the heated material showed reflections at 3.69, 3.16, 2.84, 2.62, 2.54, and 1.81 Å corresponding to the (011), ($\bar{1}$11), (111), (200), (002), and (022) *d* spacings of monoclinic ZrO_2 (ICDD card 37-1484), Figure 3c). BET analysis gave surface areas of 97 and 4 $m^2\ g^{-1}$ for the amorphous $Zr(OH)_4$ and crystalline ZrO_2 microspheres, respectively. The high surface area of the former was possibly associated with the aerosol deposition process. For example, diffusion of the water droplets during reaction and mixing at the air/water interface of the zirconium alkoxide solution, together with outflow of the alcohol byproduct of the reaction, would produce nanochannels in the wall structure of the $Zr(OH)_4$ hollow microspheres, which were subsequently removed by sintering and crystallization during heat treatment.

The above methods were extended to the fabrication of biopolymeric films comprising charged-matched polysaccharides. For this, nebulized aerosols of aqueous chitosan were directed onto the air/water interface of an alginate receiver solution to produce soft polysaccharide films that although continuous were difficult to remove as intact structures for analysis. However, high-quality films with increased stability were readily prepared by in situ calcium phosphate mineralization during interfacial deposition of the biopolymers. This was accomplished by incorporating low concentrations of calcium chloride or ammonium phosphate into the chitosan droplets or alginate receiver solution, respectively, such that electrostatic matching of the cationic and anionic polysaccharides at the air/water interface occurred concurrently with counter diffusion of the Ca^{2+} or HPO_4^{2-} ions and deposition of calcium phosphate within the incipient film. The resulting films were robust, of controllable thickness, continuous, and smooth in texture and could be lifted from the receiver solution surface and stored in distilled water as flexible mineralized biopolymeric sheets. Significantly, attempts to produce chitosan/alginate films by conventional casting methods or bulk spraying of mixtures of the two solutions produced highly irregular and aggregated gels in contrast to the well-defined high-quality films obtained by aerosol-mediated deposition.

SEM observations of washed and dried mineralized polysaccharide films collected after various deposition times showed that intact 1−2 μm diameter particles of calcium phosphate/chitosan/alginate were initially formed at the air/water interface. The number of these particles increased with time, with the consequence that the particles merged into a continuous surface coating after 20 min. The coating subsequently increased in thickness, such that self-supporting films with a flat, featureless underside, and approximately a millimeter in thickness in the hydrated state, were produced after a deposition period of 2 h (Figure 4d). FT-IR spectra confirmed the presence of the polysaccharides and calcium phosphate in the films (Figure 5d, absorption bands at 553, 573, and 1030 cm^{-1} (PO_3^{4-}), 1130 cm^{-1} (C−O−C), 1381 and 1405 cm^{-1} (COO^-), 1600 cm^{-1} (NH_3^+), 2859 and 2902 cm^{-1} (C−H), and 3480 cm^{-1} (OH)).

As chitosan/alginate composites have widespread potential in applications such as wound dressings,[21−25]— including some that are currently undergoing clinical testing,[25,26] we extended the above procedure to assess the possibility of incorporating an effective antimicrobial agent directly into the aerosol-deposited polysaccharide films during the fabrication process. As proof-of-principle, we used ultrasonic nebulization to generate chitosan droplets containing silver nanoparticles, which are known to be an effective antimicrobial agent,[27] and directed the mist onto the air/water interface of an alginate solution. The results indicated that high-quality calcium phosphate-mineralized chitosan/alginate films with well-dispersed embedded Ag nanoparticles could be readily produced (Figure 4d, Supporting Information Figure S1).

The above results demonstrate that ultrasonic nebulization can be used to generate aqueous aerosol droplets of various inorganic or organic compositions that can be subsequently directed onto the air/water interface of a range of co-reactant solutions. In each case, rapid interfacial reaction of the discrete microdroplets results in confinement of the precipitation process to a limited boundary layer around each droplet. The hollow microspheres so produced have a range of surface textures and modes of aggregation depending on the rates of diffusion and precipitation processes occurring at the air/water interface (Figure 7). In particular, coherent thin films are formed at the surface of unstirred receiver

(17) Mathiowitz, E.; Jacob, J. S.; Jong, Y. S.; Carino, G. P.; Chickering, D. E.; Chaturvedl, P.; Santos, C. A.; Vijayaraghavan, K.; Montgomery, S.; Bassett, M.; Morrell, C. *Nature* **1997**, *386*, 410.
(18) Ho, C. H.; Tobis, J.; Sprich, C.; Thomann, R.; Tiller, J. C. *Adv. Mater.* **2004**, *16*, 957.
(19) Huang, H.; Remsen, E. E. *J. Am. Chem. Soc.* **1999**, *121*, 3805.
(20) Guo, G. Y.; Chen, Y. L.; Ying, W. J. *Mater. Chem. Phys.* **2004**, *84*, 308.
(21) Piacquadio, D.; Nelson, D. B. *J. Dermatol. Surg. Oncol.* **1992**, *18*, 992.
(22) Qin, Y. M. *J. Appl. Polym. Sci.* **2006**, *100*, 2516.
(23) Biagini, G.; Bertani, A.; Muzzarelli, R. *Biomaterials* **1991**, *12*, 281.
(24) Muzzarelli, R. A. A.; Muzzarelli, C. *Adv. Polym. Sci.* **2005**, *186*, 151.
(25) Wang, L. H.; Khor, E.; Wee, A.; Lim, L. Y. *J. Biomed. Mater. Res.* **2002**, *63*, 610.
(26) Kim, H. J.; Lee, H. C.; Oh, J. S.; Shin, B. A.; Oh, C. S.; Park, R. D.; Yang, K. S.; Cho, C. S. *J. Biomater. Sci. Polym. Ed.* **1999**, *10*, 543.
(27) Parsons, D.; Bowler, P. G.; Myles, V.; Jones, S. *Wounds-Comp. Clin. Res. Prac.* **2005**, *17*, 222.

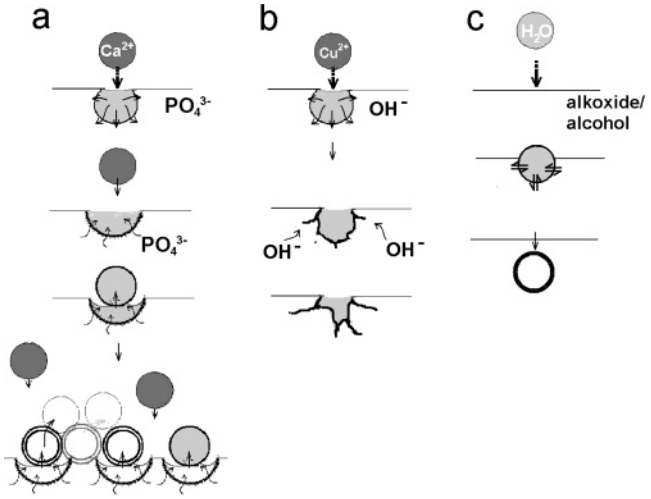

Figure 7. Sketch of suggested mechanisms of aerosol-mediated interfacial precipitation; see text for details: (a) Fast precipitation on unstirred solutions (calcium phosphate or chitosan/alginate). (b) Slow precipitation on unstirred solutions (copper hydroxide). (c) Rapid precipitation on stirred solutions (zirconium hydroxide).

solutions when the rate of interfacial precipitation is fast (Figure 7a). For example, in the case of HAP film formation, initial rapid reaction of the Ca^{2+}-containing droplets at the air/water interface of the unstirred phosphate solution results in limited spreading of the droplet away from the boundary layer and produces nanotextured hemispheres that partially increase in size by subsequent mixing with unreacted droplets. Packing of the hemispheres into a coherent underside layer occurs as the number of mineralized droplets increases, and subsequent deposition on top of this layer depends on diffusion of phosphate ions through the primary mineralized film. The latter occurs with limited dispersal of the droplets to produce a top surface consisting of aggregated arrays of hollow microspheres.

In contrast, reaction of Cu^{2+}-containing aerosol droplets at the surface of unstirred aqueous sodium hydroxide results in the relatively slow precipitation of $Cu(OH)_2$ (Figure 7b). The mineralized hemispheres disperse but complete mixing in the bulk solution does not occur. Instead, growth of the mineral phase is restricted to the air/water interface, possibly by surface tension or rapid outflowing of the droplet solution, such that nanoscale filaments of copper hydroxide are produced. Finally, rapid reaction of aerosol water droplets at the air/solution interface of a stirred ethanol/propanol solution of Zr(IV) alkoxide produces intact $Zr(OH)_4$ hollow microspheres rather than coherent thin films (Figure 7c). In this case, stirring the receiver solution displaces the mineralized droplets away from the air/water interface such that hollow zirconium hydroxide microspheres are produced in the bulk solution.

Conclusions

The flexibility of the above approach is conducive with a new general strategy for the preparation of thin films and hollow microspheres of nanostructured materials. With limitation of the extent of diffusion of the aerosol droplets at the air/water interface of the receiver solution, numerous materials with high porosity and surface area should be available using this facile method. Moreover, we have shown that the method can be readily extended to polysaccharide films and that bioactive additives such as silver nanoparticles can be embedded within the layers during fabrication, suggesting that a wide range of soft and partially mineralized biomaterials could be prepared by aerosol-mediated deposition using ultrasonic nebulization. Further studies of this new methodology are currently being made.

Acknowledgment. This work was supported by the EPSRC (Advanced Research Fellowship (D.W.), and project studentship GR/T22353 (V.S.)). We thank Elisa Boanini for assistance with surface area measurements.

Supporting Information Available: EDX analysis from mineralized polysaccharide film with intercalated Ag nanoparticles (Figure S1). This material is available free of charge via the Internet at http://pubs.acs.org.

CM0621951